

Article

3,4-Dihydroxybenzenesulfonyl-Functionalized Polyethyleneimine for Uranium Chelation

Kai Liang ^{1,2,†} , Sifan Liu ^{2,†}, Fan Zhang ^{2,3}, Wenjin Cui ^{2,4}, Ying Tian ², Shuchen Liu ^{2,*} and Lin Wang ^{1,2,*}

¹ School of Pharmacy, Guangdong Pharmaceutical University, Guangzhou 510006, China; a2724963261@163.com

² Beijing Institute of Radiation Medicine, Beijing 100850, China; 18146539471@163.com (S.L.); zhangfan201103@163.com (F.Z.); cuiwj112233@163.com (W.C.); hq6106@aliyun.com (Y.T.)

³ School of Pharmacy, Henan University, Kaifeng 475001, China

⁴ College of Chemistry and Life Science, Beijing University of Technology, Beijing 100124, China

* Correspondence: liusc118@163.com (S.L.); wanglin@bmi.ac.cn (L.W.)

† These authors contributed equally to this work.

Abstract

3,4-dihydroxybenzenesulfonyl-functionalized polyethyleneimine (PS), a novel polymeric chelator, was synthesized by conjugating 3,4-dihydroxybenzenesulfonyl (CAM) groups with branched polyethyleneimine (BPEI, MW = 600 Da) via N-acylation. PS demonstrated a high uranium adsorption capacity of 78.08% at a concentration of 4 mg/mL, accompanied by significant selectivity over competing ions such as Ca^{2+} , Zn^{2+} , and Cu^{2+} . Notably, in competitive adsorption experiments, PS exhibited a uranium adsorption rate of 59.49%, which was 3.95 times higher than that of calcium (15.06%) in the Ca^{2+} system. Cytotoxicity assays revealed enhanced biocompatibility ($\text{IC}_{50} = 86.98 \mu\text{g/mL}$), surpassing $\text{CaNa}_3\text{-DTPA}$ 3.7-fold. In a uranium exposure model (200 $\mu\text{g/mL}$), PS significantly improved cell survival rates and reduced intracellular uranium levels by 77.37% (immediate administration) and 64.18% (delayed administration). These findings establish PS as a potent and safe polymeric chelator for uranium decorporation, offering a promising strategy for mitigating the hazards of radioactive materials.

Keywords: uranium chelator; polyethyleneimine; siderophores



Academic Editor: Muhammad Salahuddin Khan

Received: 25 June 2025

Revised: 4 August 2025

Accepted: 19 August 2025

Published: 21 August 2025

Citation: Liang, K.; Liu, S.; Zhang, F.; Cui, W.; Tian, Y.; Liu, S.; Wang, L. 3,4-Dihydroxybenzenesulfonyl-Functionalized Polyethyleneimine for Uranium Chelation. *Polymers* **2025**, *17*, 2256. <https://doi.org/10.3390/polym17162256>

Copyright: © 2025 by the authors. Licensee MDPI, Basel, Switzerland. This article is an open access article distributed under the terms and conditions of the Creative Commons Attribution (CC BY) license (<https://creativecommons.org/licenses/by/4.0/>).

1. Introduction

With the wide application of nuclear technology in industry, agriculture, medicine, military, and many other fields, radiation has also become a technological double-edged sword. The trans-media migration mechanism of radionuclide uranium in the environmental-biological interface exacerbates pollution hazards. Uranium, in the form of uranyl ions (UO_2^{2+}), has a long-term presence and enters the human body through the bioconcentration effect of the food chain [1]. After entering the body, it mainly deposits in the kidneys, bones, and liver, is difficult to discharge, and triggers irreversible internal irradiation damage and metal toxicity effects [2,3].

Currently, the treatment for uranium pollution is facing the double technical bottleneck of environmental remediation and in vivo excretion promotion. Traditional chelating agents (such as DTPA) in seawater media experience reduced uranium adsorption capacity due to the interference of competing ions [4]. In vivo, they are limited by the coordination mode and find it difficult to achieve the ideal effect of promoting uranium excretion. Their use is prone to cause kidney damage and other toxic side effects [5,6]. It is challenging to

balance the coordination stability and biosafety of this linear small molecule chelator in complex media, which seriously limits its application in cross-scenario uranium contamination management. Given the many limitations of traditional chelating agents in treating uranium contamination, researchers have begun to look to polymeric materials that offer unique advantages.

Polymers offer distinct advantages over traditional small molecule chelators, primarily due to their high chelation capacity and unique biodistribution characteristics [7]. The increased number of chelation sites per unit area in polymers enhances complexation efficiency, while their larger size leads to mechanical retention by major organs, facilitating indirect targeting and improved drug delivery [8].

Branched polyethyleneimine (BPEI), a water-soluble polymer, stands out due to its high solubility [9], high capacity [10], biocompatibility [11], and indirect targeting ability [12]. These properties make it promising for diverse applications. The polyamino structure of BPEI allows surface modification via reaction with epoxide groups, acids, acyl chloride, and isocyanate. This modified BPEI can remove in vitro contaminants and promote in vivo nuclide excretion. Moreover, as a DTPA polymer derivative, BPEI has abundant chelating sites. These sites can be targeted to specific areas such as the lungs, bones, liver, or kidneys, potentially revolutionizing the field of decorporation chelating agents. Specifically, a 600 Da BPEI molecule provides approximately 14 amine coordination sites, as confirmed by potentiometric titration [13]. Molecular dynamics simulations reveal that the branched architecture of BPEI offers superior conformational flexibility compared to linear PEI (LPEI), enabling synergistic interactions between secondary and tertiary amine groups that enhance uranyl complex stability [7]. Crucially, low molecular weight BPEI (e.g., 600 Da) shows enhanced cellular internalization and reduced cytotoxicity. This is because its lower surface charge density weakens electrostatic interactions with plasma membranes, preserving membrane integrity [14]. Moreover, cytotoxicity assays indicate that 600 Da BPEI only affects cell viability at concentrations much higher than those needed for therapeutic effects [15]. This significant safety window between effective dose and cytotoxic threshold strongly supports the potential of BPEI as a versatile carrier platform for pharmaceutical development. Importantly, the preserved cellular viability at pharmacologically relevant concentrations aligns with previous optimized BPEI-based delivery systems showing enhanced biocompatibility through structural modifications [16]. In summary, BPEI demonstrates significant potential in drug development due to its multifaceted advantages. Its favorable biocompatibility and low toxicity profile further solidify its position as an excellent candidate for decorporation agent development. For example, pioneering work by Lahrouch et al. established methylcarboxylated polyethyleneimine (PEI-MC) as an effective uranium decorporation agent through multi-technique characterization (ICP-MS, FT-IR), demonstrating 0.47 mg U(VI)/mg loading capacity via mono- and bi-dentate coordination [8]. Subsequent research on polyethyleneimine-methylphosphonate (PEI-MP) further demonstrated actinide-binding capabilities, with U(VI)- and Th(IV)-loading capacities reaching 0.56–0.80 mg/mg and 0.15–0.20 mg/mg, respectively [17]. Collectively, these findings highlight the transformative potential of polymeric chelators in advancing treatments for internal radionuclide contamination.

Simultaneously, siderophores, with high Fe^{3+} binding ability, can also chelate UO_2^{2+} due to their similar coordination configurations. Given their high selectivity, low toxicity, and efficiency, siderophores are ideal chelating ligands [18]. This study innovatively designs a novel uranium chelator, PS, by grafting siderophore-specific CAM groups onto BPEI (MW = 600 Da) via N-acylation. This design aims to combine the high chelation capacity of BPEI with the high selectivity of siderophores, thereby addressing the limitations of current decorporation agents and enhancing the efficiency and safety of uranium removal. This de-

sign leverages BPEI's polyamine sites for uranium enrichment and passive targeting, while siderophore ligands precisely recognize the uranyl ion's octahedral configuration, forming a multi-level chelation network. The optimized 600 Da BPEI balances cellular uptake and biocompatibility, synergistically enhancing chelation capacity and biocompatibility, offering new insights for developing chelating agents.

2. Materials and Methods

2.1. Materials

3,4-Dimethoxybenzenesulfonyl chloride (98%) was purchased from Shanghai Titan Technology Co., Ltd. (Shanghai, China). BPEI (MW = 600 Da, 1800 Da, 10,000 Da), triethylamine (TEA, 99.5%), and boron tribromide solution (1.0 M in CH_2Cl_2) were obtained from Beijing Inokai Technology Co., Ltd. (Beijing, China). Copper(II) chloride, anhydrous zinc chloride, ferric chloride, and anhydrous calcium chloride were purchased from Anhui Senrise Technology Co., Ltd. (Hefei, China). Regenerated cellulose dialysis membranes (MWCO 500 Da) were supplied by Xi'an Youbo Biotechnology Co., Ltd. (Xi'an, China). Uranyl acetate dihydrate [$\text{UO}_2(\text{CH}_3\text{COO})_2 \cdot 2\text{H}_2\text{O}$] and $\text{CaNa}_3\text{-DTPA}$ (100 mg/mL pharmaceutical grade) were sourced from Shanghai Jizhi Biochemical Technology Co., Ltd. (Shanghai, China), and the Military Medical Research Institute (Beijing, China), respectively. All other analytical grade reagents were procured from Sinopharm Chemical Reagent Co., Ltd. (Shanghai, China) and used without further purification.

For cell experiments, U(VI) stock solution (20 mg/mL) was prepared by dissolving $\text{UO}_2(\text{CH}_3\text{COO})_2 \cdot 2\text{H}_2\text{O}$ in deionizing water, after the U(IV) working solution of 320 $\mu\text{g/mL}$ was prepared by diluting the stock solution with deionized water and filtering through the microporous membrane with 0.22 μm pore diameter before use.

2.2. Analytical Techniques

^1H NMR spectra were recorded on a Bruker ECA-400 MHz (Bruker Co., Billerica, MA, USA) spectrometer with TMS as an internal standard. Chemical shifts were in ppm (δ), and coupling constants (J) were reported in Hertz (Hz). Fourier transform infrared spectra (FT-IR) were recorded on a Nicolet iS20 spectrometer (Thermo Fisher Scientific, Waltham, MA, USA) in the 4000–400 cm^{-1} range at 4 cm^{-1} resolution; samples were prepared as KBr pellets and measured in transmission mode. Scanning electron microscope (SEM) images were recorded at 0.02–30 kV on a ZEISS GeminiSEM 300 (Carl Zeiss AG, Oberkochen, Germany) equipped with a Schottky field emission electron gun. In vitro, absorbance was measured with a full-wavelength enzyme labeler (Multiskan SkyHigh, Thermo Fisher Scientific, Waltham, MA, USA). Uranium concentration was determined by inductively coupled plasma mass spectrometry (ICP-MS) on a Thermo Fisher Scientific iCAP RQ spectrometer (Thermo Fisher Scientific, Waltham, MA, USA); samples were prepared by direct dilution with 2% HNO_3 and analyzed in kinetic-energy-discrimination (KED) mode with ^{209}Bi as the internal standard.

2.3. Synthesis of PS

The reaction was initiated by dissolving 3,4-dimethoxybenzenesulfonyl chloride (1 g, 4.22 mmol) in tetrahydrofuran (5 mL), which was subsequently added dropwise to a chilled (0 $^\circ\text{C}$) THF solution (5 mL) containing PEI (0.182 g) under continuous stirring. Triethylamine (0.05 mL) and 4-dimethylaminopyridine (2 mg) were introduced as catalytic additives. Vigorous gas evolution accompanied by precipitate formation was observed during the 4 h reaction period [19]. The resultant mixture was diluted with deionized water (40 mL) to solubilize precipitated byproducts, followed by purification through dialysis (regenerated cellulose membrane, MWCO 500 Da) until complete removal of low-molecular-

weight species was confirmed. Filtration yielded an intermediate product (0.487 g) that was subsequently dissolved in dichloromethane (10 mL). Boron tribromide (12 mL) was added dropwise to the chilled (0 °C) solution over 30 min, maintaining vigorous agitation for 6 h to ensure complete demethylation [20]. The reaction was quenched with methanol (5 mL) until gas evolution ceased, followed by solvent removal via rotary evaporation under reduced pressure. The residue was reconstituted in methanol, diluted with an equal volume of water, and subjected to secondary dialysis (MWCO 500 Da). Final purification involved repeated cold water washes (3 × 20 mL) followed by vacuum desiccation, yielding the target compound PS as a hygroscopic solid (0.048 g, 9.85% overall yield based on intermediate product mass) (Figure 1).

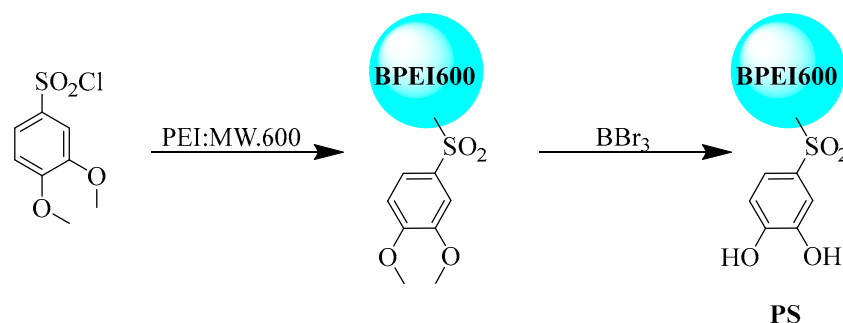


Figure 1. Two-step synthesis of sulfonamide-functionalized PS from PEI.

2.4. Adsorption of Uranium

2.4.1. Adsorption Capacity

Different masses (8, 4, 2, 1, and 0.5 mg) of PS were precisely weighed and introduced into individual 2 mL aqueous solutions containing 50 mg/L $\text{UO}_2(\text{CH}_3\text{COO})_2 \cdot 2\text{H}_2\text{O}$ to establish adsorption systems. The systems were then transferred to a thermostatic shaker and agitated at 150 rpm for 24 h at 37 °C to achieve adsorption equilibrium. Subsequently, the mixtures were centrifuged at 12,000 rpm for 15 min to separate the adsorbent from the aqueous phase. The supernatant was carefully collected, filtered through a 0.22 μm membrane to remove residual particulates, and analyzed for residual U(VI) concentration using ICP-MS. All experiments were conducted in triplicate with parallel blank controls containing no PS to ensure reproducibility and eliminate background interference.

2.4.2. Competing Adsorption Experiments

Selectivity experiments were conducted under conventional single-metal ion conditions to evaluate the adsorption performance. The experimental setup involved preparing aqueous solutions containing 50 mg/L uranium along with 250 mg/L of individual competing metal ions (Ca^{2+} , Zn^{2+} , Fe^{3+} , Cu^{2+}). For each trial, 4 mg of adsorbent material was added to 2 mL of the metal-containing uranyl solution. The adsorption systems were maintained at 37 °C in a thermostatic shaker operating at 150 rpm for 24 h to ensure equilibrium attainment. Following the adsorption phase, the mixtures underwent centrifugation at 12,000 rpm for 15 min to separate the adsorbent from the liquid phase. The supernatant was subsequently collected and analyzed for residual U(VI) concentrations using ICP-MS. All experiments were conducted in triplicate with appropriate blank controls to ensure reproducibility and minimize interference.

2.5. Cell Line and Culture

The NRK-52E cell line (organism: kidney, rat, ATCC[®], CRL-1571 DSMZ, CL-0174) was purchased from Wuhan Pricella Biotechnology Co., Ltd. (Wuhan, Hubei, China) and

was cultured in a complete medium containing DMEM (PM150210), 5% FBS (164210-50), and 1% P/S (PB180120) in a humidified atmosphere of 5% CO₂ at 37 °C. The cells were propagated every two~three days.

Cytotoxicity Assay

A cytotoxicity assay was conducted using the Cell Counting Kit-8 (CCK-8), provided by Applygen Technologies Co., Ltd., Beijing, China. The cytotoxic effects of the compounds were evaluated by determining the concentration that reduced cell growth by 50%, known as the IC₅₀ value. CaNa₃-DTPA served as a positive control in this assay. NRK-52E cells in the logarithmic growth phase were seeded into 96-well plates at a density of 5×10^3 cells per well. The plates were cultured in an incubator at 37 °C with 5% CO₂ for 24 h. The original medium was discarded, and the cells were treated with a medium containing different test compounds, whereas the blank control group received only culture media. This was followed by a further 48 h of incubation. Subsequently, 10 µL of CCK-8 solution was added to each well, and the plates were incubated for 1–2 h. The absorbance of each well at 450 nm was measured using a full-wavelength enzyme labeler. The formula used to determine the survival rate was as follows: [OD experimental]/[OD blank] 100%.

2.6. Effect of Chelating Agents on U(VI)-Induced NRK-52E Cells Injury

The therapeutic effects of the chelating agents were evaluated by modeling a 50% reduction in cell viability induced by U(VI). NRK-52E cells, in the logarithmic growth phase, were plated in 96-well plates at a density of 5×10^3 cells per well. The plates were incubated at 37 °C in an atmosphere containing 5% CO₂ for 24 h. After removal of the culture medium, the cells were concurrently exposed to 200 µg/mL UO₂(CH₃COO)₂·2H₂O and 10~80 µg/mL of the chelating agent for 48 h. Groups exposed to U(VI) only were treated with UO₂(CH₃COO)₂·2H₂O, while the blank control group was treated with culture medium alone. Subsequently, 10 µL of CCK-8 solution was added to each well, and the plates were incubated for 1–2 h. The absorbance of each well at 450 nm was measured using a full-wavelength enzyme labeler.

2.7. U(VI) Uptake and Release

In vitro U(VI) uptake and release assays were conducted to investigate the uranyl removal efficiency of PS at the cellular level. Exponentially growing NRK-52E cells were simultaneously exposed to 40 µg/mL UO₂(CH₃COO)₂·2H₂O and 5 µg/mL of the chelator. Groups exposed to U(VI) only were treated with UO₂(CH₃COO)₂·2H₂O. Additionally, control groups not exposed to U(VI) were cultured in a medium without treatment. After a 48 h incubation period, the cultured NRK-52E cells were washed with phosphate-buffered saline (PBS), trypsinized to detach them from the culture vessel, and counted using a cell counter. The cells were then subjected to microwave-assisted digestion and diluted with 5% nitric acid. The samples' U(VI) content was subsequently determined using ICP-MS. The measurements were used to determine the concentration of ²³⁸U(VI) in each sample, where the intracellular ²³⁸U(VI) content was expressed in nanograms per 10⁶ cells [21].

However, because NRK-52E cells were cultured in a medium containing uranium throughout the experiments, the primary mode of action of the ligand, whether it blocks uranium uptake by the cells or promotes the release of uranium from the cells, remains uncertain. To accurately assess the chelator's effect on promoting the release of uranium, we developed an additional in vitro method. This method involves the detection of U(VI) release from NRK-52E cells [21]. Initially, the cells were treated with a 40 µg/mL UO₂(CH₃COO)₂·2H₂O solution. The uranium-containing medium was replaced with a so-

lution containing 5 µg/mL of the chelator. The post-processing techniques and subsequent computational methods used in our study are intended to be consistent with established models of immediate drug delivery and to ensure that our findings are consistent with current scientific understanding.

2.8. Statistical Analysis

In vitro, experimental data were obtained from no fewer than three independent experiments, with each experiment including triplicate measurements. All data are presented as the mean \pm standard deviation (SD). Statistical analysis was conducted using nonlinear regression (curve fit) and one-way analysis of variance (ANOVA), as implemented in GraphPad Prism version 9.5.0. A coefficient of determination (R^2) value greater than 0.9 indicates a high degree of correspondence between the experimental data and the fitted function. Statistical significance was defined as $p < 0.05$.

3. Results

3.1. Characterizations

The FT-IR (Figure 2a) analysis confirms the successful synthesis of the PS compound. For the PEI precursor (black trace), the broad band at 3278 cm^{-1} corresponds to the N–H stretching vibration of primary and secondary amines, the sharp absorption at 756 cm^{-1} to the out-of-plane N–H bending mode, and the doublet at $2936/2804\text{ cm}^{-1}$ to aliphatic C–H stretching of the $-\text{CH}_2-$ backbone. In PS (red trace), the broad absorption band at 3270 cm^{-1} is attributed to the O–H stretching vibration of the para-substituted phenolic hydroxyl groups, with peak broadening and frequency reduction resulting from intramolecular hydrogen bonding. The sharp peak at 1608 cm^{-1} corresponds to the C=C skeletal vibration of the aromatic ring, consistent with its para-substitution pattern. Distinctive absorptions at 1293 cm^{-1} and 1145 cm^{-1} are assigned to the asymmetric and symmetric stretching vibrations of the sulfonyl group ($-\text{SO}_2-$), respectively. The S–N stretching vibration observed at 1070 cm^{-1} further corroborates the formation of the sulfonamide ($-\text{SO}_2\text{-NH}-$) moiety. The doublet at 2940 cm^{-1} and 2856 cm^{-1} arises from C–H stretching vibrations of the aliphatic chain, while the multiplet spanning $1429\text{--}1528\text{ cm}^{-1}$ encompasses overlapping C=C aromatic vibrations and C–H in-plane bending modes. Notably, the significant attenuation of the N–H bending vibration (shifted from 756 cm^{-1} in PEI to 710 cm^{-1} in PS) provides direct evidence for the integration of the amino group into the sulfonamide linkage. Collectively, the emergence of sulfonamide-specific infrared signatures (1293 , 1145 , and 1070 cm^{-1}) and the suppression of N–H bending confirm the structural integrity of PS, aligning with the designed molecular architecture. Figure 2b displays SEM micrographs of PS across sequential magnifications ($2\text{ }\mu\text{m}$ to 200 nm), revealing a hierarchical architecture with macroporous aggregates ($>50\text{ nm}$ voids), submicron particles ($200\text{--}400\text{ nm}$), and nanoscale surface defects. ^1H NMR spectra of PEI and PS (Figures S1 and S2) were acquired to verify the marked attenuation of free primary/secondary amine signals ($\delta\text{ }2.4\text{--}2.8\text{ ppm}$) and the appearance of aromatic protons ($\delta\text{ }6.84\text{--}7.30\text{ ppm}$), confirming successful conjugation and demethylation.

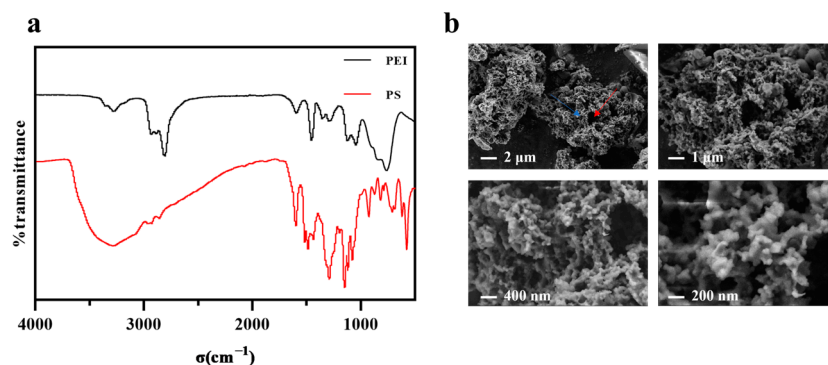


Figure 2. (a) FT-IR of PEI (black) and PS (red) highlighting characteristic vibrational bands; (b) SEM micrographs of PS at varying magnifications (red arrows indicate macroporous voids; blue arrows indicate surface defects).

3.2. Adsorption of Uranium

The *experimental* results demonstrate concentration-dependent uranium adsorption characteristics and ion-specific selectivity of PS. As shown in Figure 3a, uranium removal efficiency exhibited a progressive enhancement with increasing solid–liquid ratio, rising from 11.40% at 0.5 mg/mL to 78.08% at 4 mg/mL, with distinct saturation behavior observed beyond this threshold. Competitive adsorption studies (Figure 3b) revealed PS's preferential uranium affinity across multi-ion systems, achieving 61.25% UO_2^{2+} removal in Cu^{2+} -containing solutions despite concurrent 13.86% copper adsorption. While Fe^{3+} competition resulted in reduced uranium removal (28.37%), this primarily reflects PS's intrinsic iron-chelating functionality rather than compromised uranium selectivity, as evidenced by 50.60% Fe^{3+} adsorption attributable to structural iron-binding motifs. Notably, uranium removal consistently dominated over competitor ions in other systems, particularly in Ca^{2+} -containing solutions (59.49% U vs. 15.06% Ca^{2+} removal) and Zn^{2+} environments (51.36% U vs. 17.86% Zn^{2+} removal), confirming the material's engineered specificity for uranyl species.

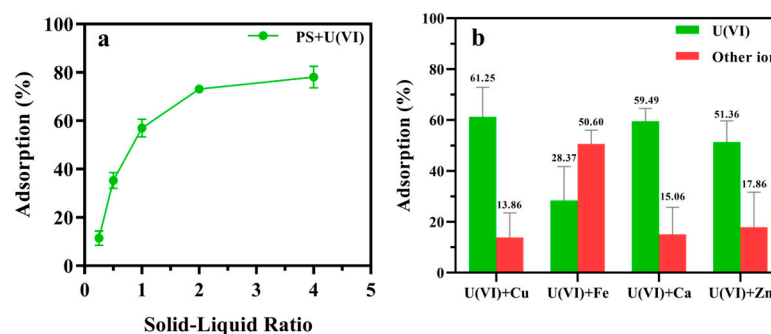


Figure 3. (a) solid–liquid ratios on adsorption of U(VI); (b) selectivity of PS toward UO_2^{2+} ion (50 mg/L) and individual interfering ion (250 mg/L) in water solution. Bars indicate SD, $n = 3$ samples.

3.3. Cytotoxicity Assay

The molecular weight-dependent biocompatibility of PEI was established through cytotoxicity screening (Figure 4a), where systematic evaluation of three variants (600, 1800, and 10,000 Da) across 62.5–1000 $\mu\text{g/mL}$ revealed an inverse correlation between molecular weight and renal cell viability. The 600 Da PEI demonstrated superior biosafety with an IC_{50} of 809.6 $\mu\text{g/mL}$ ($R^2 = 0.9289$) (Figure 4b), maintaining >80% viability at 1000 $\mu\text{g/mL}$, while intermediate (1800 Da) and high (10,000 Da) molecular weight counterparts exhibited 18.41% and 23.21% greater cytotoxicity, respectively. This molecular weight-dependent toxicity profile scientifically validates the selection of low-MW PEI (600 Da) as the optimal

precursor for PS synthesis, ensuring maximal safety margins for subsequent therapeutic applications. Building on this molecular weight optimization, renal biosafety assessment of uranium decorporation agents showed that the 600 Da PEI precursor exhibited exceptional biocompatibility, whereas its structurally modified derivative PS displayed moderate cytotoxicity ($IC_{50} = 86.98 \mu\text{g/mL}$, $R^2 = 0.9826$) (Figure 4c) within 6.25–100 $\mu\text{g/mL}$, representing a 9.3-fold tolerance reduction. In contrast, the positive control $\text{CaNa}_3\text{-DTPA}$ demonstrated substantially higher cytotoxicity ($IC_{50} = 23.61 \mu\text{g/mL}$, $R^2 = 0.9662$) (Figure 4d), with PS maintaining 3.7-fold greater viability at equivalent concentrations.

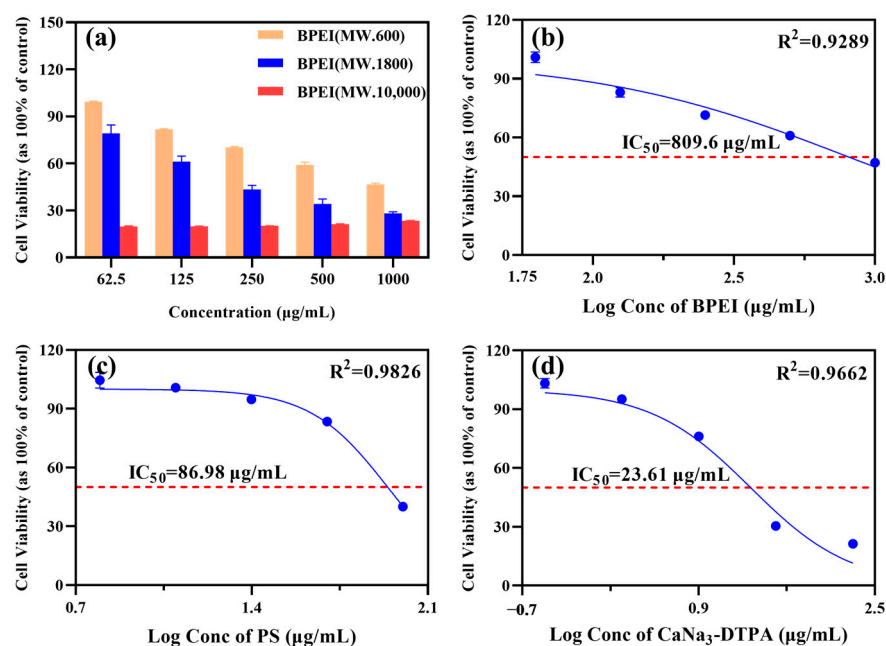


Figure 4. Dose-dependent effects on NRK-52E cell viability following treatment with (a) PEIs of varying molecular weights, (b) PEI, (c) PS, and (d) $\text{CaNa}_3\text{-DTPA}$. Bars indicate SD, $n = 3$ samples. Blue solid lines, fitted dose–response curves; red dashed lines, IC_{50} values.

The logarithmic concentration–response curves revealed strong correlations for all compounds ($R^2 > 0.90$), with PS maintaining $>60\%$ cell viability across its entire test range versus $<40\%$ survival for $\text{CaNa}_3\text{-DTPA}$ at corresponding concentrations. This comparative analysis confirms that while PS synthesis moderately increases cytotoxicity relative to native PEI, the derivative retains superior renal biosafety compared to current clinical standards, validating its potential as a uranium–chelating agent with reduced nephrotoxic risk.

3.4. Effect of Chelating Agents on U(VI)-Induced NRK-52E Cells Injury

As shown in Figure 5a, NRK-52E cells were exposed to uranyl acetate dihydrate $[\text{UO}_2(\text{CH}_3\text{COO})_2 \cdot 2\text{H}_2\text{O}]$ at concentrations ranging from 2.5 to 320 $\mu\text{g/mL}$ for 48 h. Dose–response analysis revealed an IC_{50} value of 221.7 $\mu\text{g/mL}$ ($R^2 = 0.9807$), prompting the selection of 200 $\mu\text{g/mL}$ for subsequent model construction. Figure 5b demonstrates that U(VI)-exposed controls exhibited $57.56 \pm 4.68\%$ cell viability, whereas co-treatment with the chelator PS at 20, 40, and 80 $\mu\text{g/mL}$ significantly increased viability to $72.93 \pm 7.58\%$, $89.01 \pm 1.99\%$, and $102.73 \pm 2.93\%$, respectively ($p < 0.05$ for all concentrations vs. U(VI) group). Notably, PS outperformed $\text{CaNa}_3\text{-DTPA}$ (at equivalent doses), while the precursor PEI exhibited no protective effect across the administered dose range of 10–80 $\mu\text{g/mL}$, with cell viability remaining stable between $57.71 \pm 0.38\%$ and $58.21 \pm 0.60\%$. These results indicate that PS-mediated uranium chelation reduces free U(VI) bioavailability, thereby

attenuating cytotoxicity and restoring cellular homeostasis more effectively than clinically used DTPA.

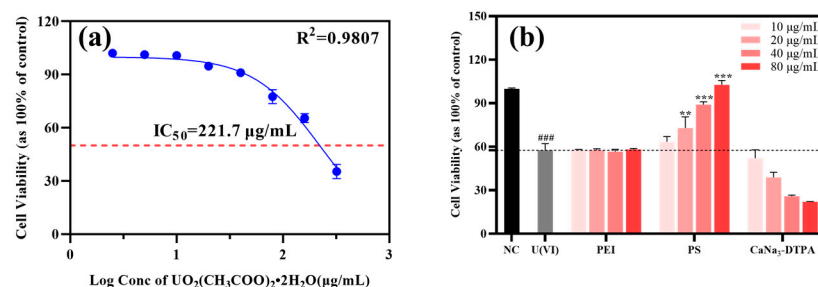


Figure 5. (a) Dose-dependent effects on NRK-52E cell growth rate following treatment with $\text{UO}_2(\text{CH}_3\text{COO})_2 \cdot 2\text{H}_2\text{O}$. (b) Effects of chelating agents on U(VI)-induced injury in NRK-52E cells. Blue solid lines, fitted dose-response curves; red dashed lines, IC_{50} values; black dashed lines, cell viability of the U(VI)-treated control. ### $p < 0.001$ compared to the control group, *** $p < 0.001$, ** $p < 0.01$ compared to the U(VI)-treated control. Bars indicate SD, $n = 3$ samples.

3.5. U(VI) Uptake and Release

Toxicity and decorporation effect are key evaluation criteria for actinide decorporation agents. This study evaluated the combined cytotoxicity of a newly synthesized chelator with uranyl ions and compared them with the commercially available decorporation agent $\text{CaNa}_3\text{-DTPA}$. Similarly, we used NRK-52E for cellular evaluation. Based on the cytotoxicity data from Figure 5a, which evaluated the effects of uranyl ions on cell viability, we determined that a concentration of 40 $\mu\text{g/mL}$ $\text{UO}_2(\text{CH}_3\text{COO})_2 \cdot 2\text{H}_2\text{O}$ would be appropriate for subsequent experiments investigating combined toxicity and U(VI) uptake and release effects.

Therefore, a comprehensive toxicity assay of U(VI) and chelating agents was performed by adding 40 $\mu\text{g/mL}$ $\text{UO}_2(\text{CH}_3\text{COO})_2 \cdot 2\text{H}_2\text{O}$ and different concentrations of chelating agents ranging from 2.5 to 40.0 $\mu\text{g/mL}$. As depicted in Figure 6a, compound PS displayed superior-combined cytotoxicity profiles at concentrations ranging from 2.5 to 40 $\mu\text{g/mL}$, with lower cytotoxicity levels than those observed for $\text{CaNa}_3\text{-DTPA}$. Notably, the cytotoxicity in the $\text{CaNa}_3\text{-DTPA}$ treatment group was pronounced at higher concentrations, resulting in a cell survival rate below 60% at doses between 10–40 $\mu\text{g/mL}$. This marked difference in overall cytotoxicity, compared to the chelating agent PS at equivalent concentrations, led us to exclude this concentration range for cellular decorporation studies.

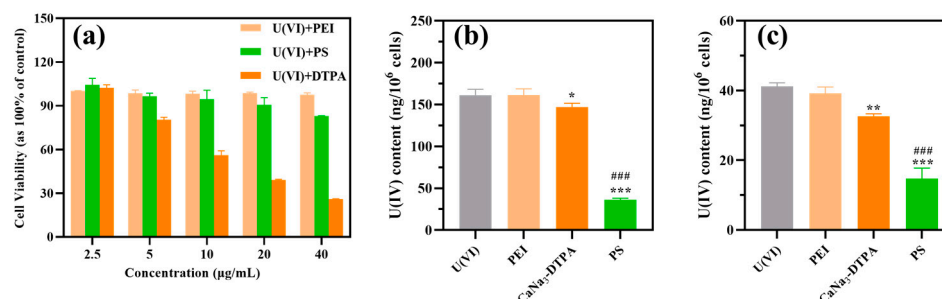


Figure 6. (a) Dosage-dependent growth rate of NRK-52E cells treated with U(VI), 40 $\mu\text{g/mL}$ + PEI, U(VI), 40 $\mu\text{g/mL}$ + PS, and U(VI), 40 $\mu\text{g/mL}$ + $\text{CaNa}_3\text{-DTPA}$; (b) Immediate administration; and (c) Delayed administration effects of PEI (5 $\mu\text{g/mL}$), PS (5 $\mu\text{g/mL}$), and $\text{CaNa}_3\text{-DTPA}$ (5 $\mu\text{g/mL}$) on the uptake and release of U(VI) in NRK-52E cells exposed to U(VI) (40 $\mu\text{g/mL}$). *** $p < 0.001$, ** $p < 0.01$, * $p < 0.05$ compared to the U(VI)-treated control. ### $p < 0.001$ compared to the $\text{CaNa}_3\text{-DTPA}$. Bars indicate SD, $n = 3$ samples.

However, at a concentration of 5 $\mu\text{g/mL}$, the cell survival rate in the $\text{CaNa}_3\text{-DTPA}$ group was $80.53 \pm 1.67\%$, which was comparable to the cytotoxicity of chelator PS at the same concentration, all exhibiting low cytotoxicity. This similarity in cytotoxicity at concentrations below 5 $\mu\text{g/mL}$ suggests that chelator PS has a similar safety profile to $\text{CaNa}_3\text{-DTPA}$. Consequently, a concentration of 5 $\mu\text{g/mL}$ was selected as the cellular decorporation evaluation concentration for assessing the decorporation efficacy of the chelating agents. To determine the principal mode of action of the chelating agent in the context of uranium toxicity, we established two distinct delivery models (immediate and delayed). The first model involved immediate administration of the chelating agent to assess its ability to block uranium uptake by cells. The second model was designed to examine the agent's efficacy in promoting the release of uranium from cells when delivered after an initial exposure period. These models provided a framework for understanding the agent's role in mitigating uranium entry or enhancing its elimination from cells.

As demonstrated in Figure 6b,c, compound PS exhibited significant uranium removal efficacy in both administration models. Under immediate administration conditions, PS reduced U(VI) levels by 77.37% compared to the U(VI)-treated group, while $\text{CaNa}_3\text{-DTPA}$ achieved only an 8.7% reduction under identical parameters. In delayed administration scenarios, PS maintained superior performance with a 64.18% decrease in U(VI) content relative to the control group, whereas $\text{CaNa}_3\text{-DTPA}$ showed limited efficacy with a 20.86% reduction. These results conclusively demonstrate that PS outperforms the positive control drug $\text{CaNa}_3\text{-DTPA}$ in uranium elimination efficiency under equivalent mass concentration dosing conditions, regardless of administration timing (immediate or delayed).

4. Discussion

This study successfully developed and evaluated a novel polymeric chelator, PS, based on low-molecular-weight BPEI modified with 3,4-dimethoxybenzenesulfonyl groups, for enhanced uranium decorporation. The design rationale centered on leveraging the high chelation capacity of BPEI's three-dimensional architecture and integrating sulfonamide functionalities to improve uranyl coordination and cellular permeability. Key findings demonstrate that PS exhibits superior uranium adsorption efficiency, selectivity, and biocompatibility compared to the positive control drug $\text{CaNa}_3\text{-DTPA}$, addressing critical limitations of current decorporation therapies.

Compared with traditional small molecule chelators like $\text{CaNa}_3\text{-DTPA}$ and EDTA, PS shows significant advantages in uranium adsorption capacity and selectivity. For example, in a study by Leydier et al. [4], EDTA- and DTPA-modified ligands were investigated as sequestering agents for uranyl decorporation. Their results showed that these traditional chelators had reduced uranium adsorption capacity in seawater media due to the interference of competing ions. In contrast, PS demonstrated a high uranium adsorption capacity of 78.08% at a concentration of 4 mg/mL, with significant selectivity over competing ions such as Ca^{2+} , Zn^{2+} , and Cu^{2+} . This superior adsorption capacity and selectivity of PS can be attributed to its unique design combining the high chelation capacity of BPEI and the high selectivity of siderophores.

In terms of biocompatibility, PS also outperforms traditional chelators. As mentioned in the study by Muller et al. [6], the use of DTPA for uranium decorporation is prone to cause kidney damage and other toxic side effects. However, cytotoxicity assays in our study revealed that PS had an IC_{50} of 86.98 $\mu\text{g/mL}$, which is 3.7-fold higher than that of $\text{CaNa}_3\text{-DTPA}$ (23.61 $\mu\text{g/mL}$). This enhanced biosafety likely stems from the branched BPEI backbone, which mitigates membrane disruption by reducing surface charge density. For instance, Lahrouch et al. [8] reported that methylcarboxylated polyethyleneimine (PEI-MC) exhibited good biocompatibility and was effective as a uranium decorporation agent. Our

PS, with its optimized molecular weight and introduced sulfonamide moieties, further improves the balance between chelation efficacy and biocompatibility.

Moreover, PS shows better performance in reducing intracellular uranium levels compared to traditional chelators. In a uranium exposure model (200 µg/mL), PS significantly improved cell survival rates and reduced intracellular uranium levels by 77.37% (immediate administration) and 64.18% (delayed administration). In comparison, CaNa₃-DTPA achieved only an 8.7% reduction in immediate administration and a 20.86% reduction in delayed administration scenarios. This indicates that PS is more effective in mitigating the hazards of uranium exposure at the cellular level. The observed selectivity of PS for uranium over competing ions, particularly in Ca²⁺-rich environments, is critical for clinical translation, as calcium displacement by traditional chelators like DTPA often exacerbates nephrotoxicity [22]. Furthermore, the hierarchical porosity of PS, as revealed by SEM, likely facilitates intracellular uranium sequestration through enhanced diffusion and surface interactions [23]. The reduced cytotoxicity of low-MW BPEI (600 Da) compared to higher-MW variants aligns with previous reports attributing toxicity to excessive electrostatic interactions with cellular membranes [24]. By optimizing molecular weight and introducing sulfonamide moieties, this study achieves a balance between chelation efficacy and biocompatibility, a critical advancement in polymeric chelator design.

Despite the promising results, this study has certain limitations. The evaluations were conducted exclusively *in vitro*, and future research should validate the efficacy and safety of PS in animal models to assess pharmacokinetics, biodistribution, and long-term safety. This will be crucial for the clinical translation of PS as a potential uranium decorporation agent. Additionally, the competitive adsorption experiments focused on individual ions rather than complex biological matrices, which may better simulate *in vivo* conditions. Future studies should explore PS's decorporation efficacy *in vivo*, investigate its renal clearance profile, and evaluate potential off-target interactions with essential metal ions.

5. Conclusions

We have translated the concept of a “polymer–siderophore hybrid” into a readily accessible molecule, PS, that achieves gram-scale production in two straightforward steps without costly catalysts or chromatography. The material displays record-high uranium removal under mild, near-physiological conditions—78% extraction at 4 mg/mL within 24 h—and retains more than half of this performance even when challenged by a five-fold excess of competing earth-abundant cations, a scenario typical of seawater or blood serum. Equally important, its cytotoxicity threshold lies 3.7-fold above that of the clinical standard CaNa₃-DTPA, while a single 5 µg/mL dose lowers intracellular uranium by 64–77% irrespective of whether administration is immediate or delayed. These metrics collectively indicate that PS can operate effectively at concentrations at least one order of magnitude below those required by current chelators, sharply reducing the risk of nephrotoxicity and easing dosing regimens. Because the underlying branched PEI scaffold is already produced industrially and the catechol-sulfonamide ligand is derived from inexpensive commodity chemicals, the route is inherently scalable; the absence of precious metals or protecting-group manipulations keeps projected costs well below those of other advanced adsorbents or decorporation agents. Consequently, PS is positioned to bridge laboratory discovery with real-world deployment—whether as packed-bed cartridges for groundwater treatment, membrane coatings for seawater mining, or injectable therapeutics for accidental exposure—offering a single platform that addresses both environmental cleanup and human health protection without the compromises that have so far limited existing technologies.

Supplementary Materials: The following supporting information can be downloaded at the following address: <https://www.mdpi.com/article/10.3390/polym17162256/s1>. Figure S1. ¹H-NMR spectrum of PEI (600 Da) in DMSO-d₆. Figure S2. ¹H-NMR spectrum of PS in DMSO-d₆.

Author Contributions: Conceptualization, S.L. (Shuchen Liu) and L.W.; methodology, K.L. and S.L. (Sifan Liu); investigation, F.Z., K.L. and W.C.; resources, W.C.; validation, L.W.; data curation, Y.T.; writing—original draft preparation, K.L. and S.L. (Sifan Liu); writing—review and editing, L.W. and S.L. (Shuchen Liu). All authors have read and agreed to the published version of the manuscript.

Funding: This research received no external funding.

Institutional Review Board Statement: The NRK-52E cell line was obtained from Wuhan Pricella Biotechnology Co., Ltd.

Data Availability Statement: The original contributions presented in this study are included in the article/Supplementary Material. Further inquiries can be directed to the corresponding author.

Conflicts of Interest: The authors declare no conflict of interest.

References

- Chen, L.; Liu, J.; Zhang, W.; Zhou, J.; Luo, D.; Li, Z. Uranium (U) source, speciation, uptake, toxicity and bioremediation strategies in soil-plant system: A review. *J. Hazard. Mater.* **2021**, *413*, 125319. [CrossRef] [PubMed]
- Vicente-Vicente, L.; Quiros, Y.; Pérez-Barriocanal, F.; López-Novoa, J.M.; López-Hernández, F.J.; Morales, A.I. Nephrotoxicity of Uranium: Pathophysiological, Diagnostic and Therapeutic Perspectives. *Toxicol. Sci.* **2010**, *118*, 324–347. [CrossRef]
- Gritsaenko, T.; Pierrefite-Carle, V.; Lorivel, T.; Breuil, V.; Carle, G.F.; Santucci-Darmanin, S. Natural uranium impairs the differentiation and the resorbing function of osteoclasts. *Biochim. Biophys. Acta (BBA)—Gen. Subj.* **2017**, *1861*, 715–726. [CrossRef]
- Leydier, A.; Lin, Y.; Arrachart, G.; Turgis, R.; Lecerclé, D.; Favre-Reguillon, A.; Taran, F.; Lemaire, M.; Pellet-Rostaing, S. EDTA and DTPA modified ligands as sequestering agents for uranyl decorporation. *Tetrahedron* **2012**, *68*, 1163–1170. [CrossRef]
- Ansoborlo, E.; Prat, O.; Moisy, P.; Auwer, C.D.; Guilbaud, P.; Carriere, M.; Gouget, B.; Duffield, J.; Doizi, D.; Vercouter, T.; et al. Actinide speciation in relation to biological processes. *Biochimie* **2006**, *88*, 1605–1618. [CrossRef]
- Muller, D.; Houpert, P.; Napoli, M.H.; Métivier, H.; Paquet, F. Synergie potentielle entre deux toxiques rénaux: Le DTPA et l'uranium. *Radioprotection* **2006**, *41*, 413–420. [CrossRef]
- Kobayashi, S.; Hiroishi, K.; Tokunoh, M.; Saegusa, T. Chelating properties of linear and branched poly(ethylenimines). *Macromolecules* **1987**, *20*, 1496–1500. [CrossRef]
- Lahrouch, F.; Chamayou, A.C.; Creff, G.; Duvail, M.; Hennig, C.; Rodriguez, M.J.L.; Auwer, C.D.; Di Giorgio, C. A Combined Spectroscopic/Molecular Dynamic Study for Investigating a Methyl-Carboxylated PEI as a Potential Uranium Decorporation Agent. *Inorg. Chem.* **2017**, *56*, 1300–1308. [CrossRef]
- Yang, Y.; Liu, X.; Yang, C.; Wang, Y.; Fan, H. Adsorption of hydrogen sulfide by MOFs loaded with polyethyleneimine (PEI). *J. China Coal Soc.* **2024**, *49*, 3225–3234.
- Mei, S.; Yang, J.; Zhang, Q.; Zhao, F.; Yuan, J.; Hui, F.; Lv, J. Research progress on application of polyethyleneimine in the new field. *New Chem. Mater.* **2017**, *45*, 30–32+36.
- Sabin, J.; Alatorre-Meda, M.; Miñones, J.; Domínguez-Arca, V.; Prieto, G. New insights on the mechanism of polyethylenimine transfection and their implications on gene therapy and DNA vaccines. *Colloids Surf. B Biointerfaces* **2022**, *210*, 112219. [CrossRef] [PubMed]
- Hu, L.; Li, J.; Yu, C.; Du, Y.; Song, M.; Zhang, B. Research advances of polyethylenimine-based nanosystems for gene delivery. *Chin. J. Hosp. Pharm.* **2024**, *44*, 853–858.
- Jäger, M.; Schubert, S.; Ochrimenko, S.; Fischer, D.; Schubert, U.S. Branched and linear poly(ethylene imine)-based conjugates: Synthetic modification, characterization, and application. *Chem. Soc. Rev.* **2012**, *41*, 4755. [CrossRef] [PubMed]
- Jiang, C.; Wang, Y.; Xiao, H.; Zhao, H.; Liu, Q. Recent progress of non-viral vector polyethylenimine in the application of gene delivery. *Yao Xue Xue Bao* **2020**, 2869–2882. [CrossRef]
- Foxley, M.A.; Wright, S.N.; Lam, A.K.; Friedline, A.W.; Strange, S.J.; Xiao, M.T.; Moen, E.L.; Rice, C.V. Targeting Wall Teichoic Acid in Situ with Branched Polyethylenimine Potentiates β -Lactam Efficacy against MRSA. *ACS Med. Chem. Lett.* **2017**, *8*, 1083–1088. [CrossRef]
- Li, X.; Zuo, Y.; Lin, X.; Guo, B.; Jiang, H.; Guan, N.; Zheng, H.; Huang, Y.; Gu, X.; Yu, B.; et al. Develop Targeted Protein Drug Carriers through a High-Throughput Screening Platform and Rational Design. *Adv. Healthc. Mater.* **2024**, *13*, 2401793. [CrossRef]

17. Lahrouch, F.; Sofronov, O.; Creff, G.; Rossberg, A.; Hennig, C.; Auwer, C.D.; Di Giorgio, C. Polyethyleneimine methylphosphonate: Towards the design of a new class of macromolecular actinide chelating agents in the case of human exposition. *Dalton Trans.* **2017**, *46*, 13869–13877. [[CrossRef](#)]
18. Albelda-Berenguer, M.; Monachon, M.; Joseph, E. Siderophores: From natural roles to potential applications. *Adv. Appl. Microbiol.* **2019**, *106*, 193–225.
19. Wang, E.; Lv, X.; Liu, S.; Dong, Q.; Li, J.; Li, H.; Su, B. A Selective Separation Mechanism for Mono/divalent Cations and Properties of a Hollow-Fiber Composite Nanofiltration Membrane Having a Positively Charged Surface. *Membranes* **2023**, *14*, 1. [[CrossRef](#)]
20. Kosak, T.M.; Conrad, H.A.; Korich, A.L.; Lord, R.L. Ether Cleavage Re-Investigated: Elucidating the Mechanism of BBr₃-Facilitated Demethylation of Aryl Methyl Ethers. *Eur. J. Org. Chem.* **2015**, *2015*, 7460–7467. [[CrossRef](#)]
21. Wang, X.; Dai, X.; Shi, C.; Wan, J.; Silver, M.A.; Zhang, L.; Chen, L.; Yi, X.; Chen, B.; Zhang, D.; et al. A 3,2-Hydroxypyridinone-based Decorporation Agent that Removes Uranium from Bones In Vivo. *Nat. Commun.* **2019**, *10*, 2570. [[CrossRef](#)]
22. Liu, Y.; Zhao, B.; He, P.; Wang, Z.; Tang, K.; Mou, Z.; Tan, Y.; Wu, L.; Chen, G.; Li, X.; et al. Cinnamic Acid: A Low-Toxicity Natural Bidentate Ligand for Uranium Decorporation. *Inorg. Chem.* **2024**, *63*, 7464–7472. [[CrossRef](#)] [[PubMed](#)]
23. Liu, Y.; Ni, S.; Wang, W.; Zhao, Y.; Meng, Y.; Liu, H.; Yang, L. Facile and scalable synthesis of functionalized hierarchical porous polymers for efficient uranium adsorption. *Water Res.* **2024**, *257*, 121683. [[CrossRef](#)] [[PubMed](#)]
24. Bruno, K. Using drug-excipient interactions for siRNA delivery. *Adv. Drug Deliv. Rev.* **2011**, *63*, 1210–1226. [[CrossRef](#)] [[PubMed](#)]

Disclaimer/Publisher's Note: The statements, opinions and data contained in all publications are solely those of the individual author(s) and contributor(s) and not of MDPI and/or the editor(s). MDPI and/or the editor(s) disclaim responsibility for any injury to people or property resulting from any ideas, methods, instructions or products referred to in the content.